A Deconvolution Method for the Separation of Specific Versus Nonspecific Interactions in Noncovalent Protein-Ligand Complexes Analyzed by ESI-FT-ICR Mass Spectrometry

Thorsten Daubenfeld, Anne-Pascale Bouin, and Guillaume van der Rest
Laboratoire des Mécanismes Réactionnels, Ecole Polytechnique, Palaiseau, France

A method to separate specific and nonspecific noncovalent interactions observed in ESI mass spectra between a protein and its ligands is presented. Assuming noncooperative binding, the specific ligand binding is modeled as a statistical distribution on identical binding sites. For the nonspecific fraction we assume a statistical distribution on a large number of "nonspecific" interacting sites. The model was successfully applied to the noncovalent interaction between the protein creatine kinase (CK) and its ligands adenosine diphosphate (ADP) and adenosine triphosphate (ATP) that both exhibit nonspecific binding in the mass spectrum. The two sequential dissociation constants obtained by applying our method are $K_{1,diss} = 11.8 \pm 1.5$ μM and $K_{2,diss} = 48 \pm 6$ μM for ADP. For ATP, the constants are $K_{1,diss} = 27 \pm 7$ μM and $K_{2,diss} = 114 \pm 27$ μM. All constants are in good correlation with reported literature values. The model should be valuable for systems with a large dissociation constant that require high ligand concentrations and thus have increased potential of forming nonspecific adducts. (J Am Soc Mass Spectrom 2006, 17, 1239–1248) © 2006 American Society for Mass Spectrometry

The function of most, if not all, proteins is defined by their interaction with ligands (e.g., other proteins, DNA, RNA, small metabolites). These interactions are mediated by noncovalent interactions (hydrogen bonds, ionic and van der Waals as well as hydrophobic interactions). To understand the biological role of a protein, it is important to obtain detailed information about these interactions.

Electrospray ionization (ESI) mass spectrometry [1] has gained interest as a rapid and sensitive tool to derive binding constants for noncovalent interactions [2–6]. The main advantages of the mass spectrometry (MS) based approach are its sensitivity (only fmol of protein are needed), the high mass accuracy, and the possibility to obtain direct information about the stoichiometry of biomolecular complexes. However, one has to keep in mind that when using MS based methods, the observation of the interaction in question is made in the gas phase. The solution phase equilibria, thus could have been significantly altered upon transfer to the gas phase due to the modified energetic environment (like the increase of ionic interactions and loss of hydrophobic interactions in the vacuum). One of the main problems encountered in the MS approach is the binding of ligands upon transfer of the analyte to the gas phase, thus giving rise to so-called nonspecific interactions [7–14] that alter the initial (i.e., solution phase) stoichiometry of the complex (e.g., due to increase of ligand concentration during the evaporation of the droplet in the ESI process). In such a case, the gas-phase observation does not directly reflect the liquid phase equilibrium. In general, nonspecific interactions may arise when a large excess of ligand is employed, as it becomes necessary for systems with weak binding constants ($K_{diss} > 1$ μM). To study systems with weak binding constants, it is thus necessary to find means to separate specific from nonspecific binding. As both specific and nonspecific complexes have the same molecular mass, it is not possible to differentiate between them directly from the mass spectrum. One possibility to separate specific and nonspecific interactions might be to detach the nonspecifically bound ligands from the protein in the gas phase, for example by using blackbody infrared radiation dissociation (BIRD) [11]. However, this approach only yields reasonable results if the gas-phase interaction of the protein with the specifically bound ligands is much stronger than its interaction with the nonspecifically bound ligands [8]. Klassen and coworkers have shown an example of a complex containing specific and nonspecific interactions where nonspecific binding is stronger than specific binding [9]. It is thus not

Published online June 21, 2006
Address reprint requests to Dr. G. van der Rest, Laboratoire des Mécanismes Réactionnels, CNRS UMR 7651, Ecole Polytechnique, 91128 Palaiseau Cedex, France. E-mail: gvdr@dcmr.polytechnique.fr

1044-0305/06/$32.00
doi:10.1016/j.jasms.2006.05.005

Received November 24, 2005
Revised May 2, 2006
Accepted May 12, 2006

generally possible to separate a mixture of specific and nonspecific interactions using mass spectrometry techniques alone.

The phenomenon of nonspecific binding was encountered in the course of a study centered on the noncovalent interaction between rabbit muscle creatine kinase (CK) and its physiological ligands adenosine diphosphate (ADP) and adenosine triphosphate (ATP). CK is an 86 kDa homodimeric protein that is involved in the energy balance of muscle cells by catalyzing the following reaction: creatine + ATP ⇌ phosphocreatine + ADP.

CK has been extensively studied by traditional biochemical techniques since the 1960s [15] and a comprehensive review of the studies would be beyond the scope of this article. However, two elements are worth notice: it has been established that CK has two binding sites. The binding constants of the CK/ADP interaction reported cover a wide range of values ($K_{diss,ADP}$ ranging from 0.5 μM to 500 μM [15–20]). The binding constants show a dependence on the presence of other molecular species (such as Mg^{2+} or creatine) that are involved in the biological role of the protein. However, most of the reported literature values, especially those obtained in the absence of other ligand, are in the range of 70–140 μM [17–20]. For ATP, the interaction with CK has been found to be less strong, the dissociation constant being around 300–500 μM [20]. However, for both ligands, it is not yet clear if the two binding sites are cooperative or not.

It was thus of interest to probe the noncovalent interaction between CK/ADP and CK/ATP, through the use of a MS technique that allows for the simultaneous determination of the binding constant for both sites.

The ESI MS observations on the CK/ADP solutions as well as the CK/ATP solutions showed evidence for nonspecific binding. To determine the specific binding constants, we built a mathematical model that allows deconvolution between specific and nonspecific interactions. This allowed the determination of the two binding constants. The model is based on a binomial distribution of ligands on two putative specific binding sites and a Poisson distribution of ligands on putative nonspecific binding sites. The latter distribution, which has also been reported for protein-carbohydrate interactions [10], proved to be a good approximation for a system with a number as small as 10 nonspecific binding sites and should be applicable to systems exhibiting similar behavior.

Experimental

Materials

Rabbit muscle creatine kinase (CK) was obtained from Roche (Mannheim, Germany) and desalted using Micro Bio-Spin 30 columns (BioRad, Hercules, CA) with a 40 kDa MW cutoff equilibrated with 10 mM NH_4HCO_3 (pH 7.9), giving stock solutions of 200 μM protein. ADP and ATP were obtained from Sigma (St. Louis, MO) and desalted using a BioRad AG50WX8 ion-exchange resin. ADP solutions (10 mM in MilliQ grade water, Millipore, Bedford, MA) were stored at −20 °C. ATP solutions were freshly prepared daily. The concentration of the ligand stock solution was adjusted to 200 μM with 10 mM NH_4HCO_3 (pH 7.9) prior to titration experiments.

Mass Spectrometry

Experiments were preformed on a Bruker APEX III FT-ICR mass spectrometer (Bremen, Germany) equipped with a 7.0 T actively shielded magnet and an unmodified Apollo electrospray source. Titration experiments were performed by preparing solutions containing 4 μM CK and ligand concentration ranging from 1 μM to 60 μM in 10 mM NH_4HCO_3. Each point was at least repeated three times. Samples were introduced by direct infusion electrospray ionization with a flow rate of 1.5 μL/min. Instrumental parameters were adjusted to optimize detection of high *m/z* species and to preserve the noncovalent interaction between the protein subunits and between the protein and its ligands, respectively. Various conditions were tried (see Results and Discussion) and the typical changes compared with standard instrumental conditions are as follows: increase of the capillary exit voltage (250 V), increase of the hexapole radiofrequency (rf) amplitude, increase of the excitation parameters and increase of the gated-trapping delay. The nebulizing gas temperature was left at 140 °C.

ADP or ATP binding to CK results in a less than 1% change in the molecular mass of the protein. This might affect the local structure around the protein's active site, but is not assumed to significantly alter its ionization and detection efficiencies during the MS measurement (however, this assumption has to be validated for each protein-ligand system in question as some ligands may have a significant effect on the physicochemical properties of the protein). Under this assumption, the intensities in the mass spectrum reflect the relative concentrations in solution. The normalized intensities can thus be used to calculate the dissociation constant, K_i according to eq 1 [9]:

$$K_i = \frac{[P]_{eq}[L]_{eq}^{\,i}}{[PL_i]_{eq}} = \frac{\left([L]_0 - [P]_0 \cdot \sum_{j=1}^{i} j \cdot R_j \Big/ \left(1 + \sum_{j=1}^{i} jR_j\right)\right)^i}{R_i} \quad (1)$$

Here, $[P]_{eq}$, $[L]_{eq}$, and $[PL_i]_{eq}$ are the solution phase equilibrium concentrations of protein, ligand, and the complex, respectively. $[L]_0$ and $[P]_0$ are the initial concentrations of ligand and protein, respectively, *i* is the number of bound ligands and R_j is the ratio of the peak heights of the signals corresponding to the protein complex with *j* ligands and the free protein, respectively.

Deconvolution Model

In the presence of nonspecific interactions, the experimentally measured ratios R_i include contributions from both specific and nonspecific complexes. They can be represented as a sum of different contributions (eq 2):

$$R_i = \frac{I_i^0}{I_0^0} + \frac{I_i^1}{I_0^0} + \ldots + \frac{I_i^i}{I_0^0} = R_i^0 + R_i^i + \ldots + R_i^i = \sum_{j=0}^{i} R_i^j \qquad (2)$$

where I_i^j and R_i^j are, respectively, the intensity and the intensity ratio for the species with i bound ligands of which j ligands are specifically bound. As the value for R_i contains contributions from both specific and nonspecific interactions, eq 1, cannot be employed on them to determine the binding constants for the specific interactions. To obtain correct equilibrium binding constants, the sum of the specific contributions (which will be denoted R_j^*) has to be used (eq 3):

$$R_j^* = \frac{I_j^j}{\sum_{i=0}^{\infty} I_i^0} + \frac{I_{j+1}^j}{\sum_{i=0}^{\infty} I_i^0} + \frac{I_{j+2}^j}{\sum_{i=0}^{\infty} I_i^0} + \ldots = \frac{I_0^0}{\sum_{i=0}^{\infty} I_i^0} =$$

$$\left(R_j^j + R_{j+1}^j + R_{j+2}^j + \ldots\right) \cdot \frac{\sum_{i=j}^{\infty} R_i^j}{\sum_{i=0}^{\infty} R_i^0} \qquad (3)$$

Assuming statistical binding for both the specific and the nonspecific interactions, we can model the ligand binding as a convolution of two distributions. First, a binomial distribution on a limited number of specific binding sites (corresponding to specific ligand binding) and second, a statistical distribution on a large number of binding sites (corresponding to nonspecific ligand binding), as similar Poisson-type distribution was observed for nonspecific interactions under similar experimental conditions [10]. Denoting the average number of specifically occupied binding sites with $\bar{s}$ and considering that the ligand binding follows a binomial distribution, one can calculate the probability of the protein having j ligands bound specifically (P_j^{spec}) on a finite number of specific binding sites, s, relative to the probability of the protein having no specifically bound ligand (P_0^{spec}) according to eq 4:

$$\frac{P_j^{spec}}{P_0^{spec}} = \frac{s!}{j! \cdot (s-j)!} \cdot \left(\frac{\bar{s}/s}{1-\bar{s}/s}\right)^j \qquad (4)$$

A similar approach can be followed for the nonspecifically bound ligands: denoting the average number of nonspecifically occupied binding sites with $\bar{n}$, the corresponding probability of the protein having k ligands (with $k = i - j$) bound nonspecifically ($P_{\mathbf{k}}^{ns}$) on a defined number of nonspecific binding sites, n, relative to the probability of the protein having no nonspecifically bound ligands can be calculated using eq 5:

$$\frac{P_{\mathbf{k}}^{ns}}{P_0^{ns}} = \frac{n!}{k! \cdot (n-k)!} \cdot \left(\frac{\bar{n}/n}{1-\bar{n}/n}\right)^k \approx \frac{\bar{n}^k}{k!} \qquad (5)$$

In this latter case, the number of nonspecific binding sites cannot be assumed a priori. However, if the number of binding sites n is sufficiently large and if the ratio $\bar{n}/n$ is sufficiently small (which means that relatively few ligands occupy the potential binding sites), this limitation can be overcome by the approximation in the last part of eq 5. This approximation is equivalent to assuming that nonspecifically bound ligands follow a Poisson distribution. The validity of this approximation will be discussed in the "Results and Discussion" section.

The convolution between specific and nonspecific contributions is given by the product of these probabilities in eq 6:

$$R_i^j = \frac{P_j^{spec}}{P_0^{spec}} \frac{P_{i-j}^{ns}}{P_0^{ns}}$$

$$= \frac{s!}{j!\,(s-j)!} \cdot \left(\frac{\bar{s}/s}{1-\bar{s}/s}\right)^j \frac{n!}{(i-j)! \cdot (n-i+j)!} \cdot$$

$$\left(\frac{\bar{n}/n}{1-\bar{n}/n}\right)^{i-j}$$

$$\approx \frac{s!}{j!\,(s-j)!} \left(\frac{\bar{s}/s}{1-\bar{s}/s}\right)^j \frac{\bar{n}^{i-j}}{(i-j)!} \qquad (6)$$

In this expression, R_i^j only depends of four variables: s, the number of specific binding sites, $\bar{s}$, the average number of specifically bound ligands, n, the number of nonspecific binding sites, and $\bar{n}$, the average number of nonspecifically bound ligands. The numbers of specific and nonspecific binding sites are conditions that depend on the system under consideration: the first one (s) requires a priori knowledge or clear experimental evidence, the second one (n), being much more difficult to evaluate and usually not known a priori, has to be approximated somehow. This is the reason for which the Poisson approximation was used and proved useful as will be shown in the following section. $\bar{s}$ and $\bar{n}$ are related to the experimentally obtained average number of ligands $\bar{l}$ through eq 7:

$$\bar{l} = \bar{s} + \bar{n} \qquad (7)$$

By combining equations 2, 6, and 7, the experimentally measured ratios R_i can be expressed as a function of s, n, $\bar{l}$ and $\bar{s}$ (eq 8) and under the conditions stated above these ratios can be approximated as a function of s, $\bar{l}$, and $\bar{s}$.

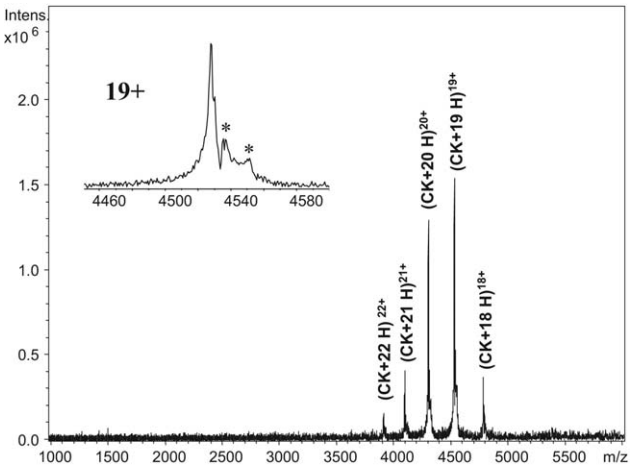

Figure 1. 4 μM CK in 10 mM NH_4HCO_3. The inset shows the charge state 19+ with adducts that were not removed during desalting and the electrospray process (asterisk).

$$R_i = \sum_{j=0}^{i} R_i^j = \sum_{j=0}^{i} \frac{s!}{j!\,(s-j)!}\left(\frac{\bar{s}/s}{1-\bar{s}/s}\right)^j \frac{n!}{(i-j)!\cdot(n-i+j)!}\cdot \left(\frac{(\bar{l}-\bar{s})/n}{1-(\bar{l}-\bar{s})/n}\right)^{i-j} \approx \sum_{j=0}^{i} \frac{s!}{j!\,(s-j)!}\left(\frac{\bar{s}/s}{1-\bar{s}/s}\right)^j \frac{(\bar{l}-\bar{s})^{i-j}}{(i-j)!} \quad (8)$$

$\bar{s}$ can be used as an adjustable parameter to fit the experimentally observed distribution at each ligand concentration used. Corrected ratios R_j^* are then obtained straightforward by reinserting the R_i^j obtained by eq 6 into eq 3. The corrected values for the ratios for the specifically bound ligands (R_j^*) obtained by this procedure can then be used to obtain the equilibrium dissociation constants by applying eq 1.

Results and Discussion

The mass spectrum of 4 μM CK in 10 mM NH_4HCO_3 buffer (pH 7.9) shows a series of peaks that can be attributed to a charge state distribution of the creatine kinase (CK) homodimer with charge states ranging from 22+ to 18+ (Figure 1). Thus, the interaction between the monomers is conserved upon transfer of the complex to the gas phase. The mass as determined by the experiment is 85,929 Da which is in good agreement with the theoretical average mass (85,943 Da). Proteins analyzed by ESI-MS under denatured conditions exhibit large bell-shaped charge state distributions [21]. On the other hand, narrow charge state distributions at relatively high *m/z*, as observed in our experiments, are believed to reflect at least a nondenatured, if not native-like structure, as originally proposed by Chowdhury and coworkers [22].

When titrated with ADP in solution, ESI-MS of the resulting complexes yielded essentially the same charge states as in the case of the homodimer with additional peaks appearing that correspond to the ligand-bound CK (Figure 2). However, the ligand-bound forms of CK displayed a slightly higher charge state than the free protein, manifesting itself in a variation of ligand occupancy between different charge states in the spectrum (Figure 2, middle and bottom). The phenomenon of charge state variation between free and ligand-bound forms of the protein has been observed and described by Wang and coworkers [9] and seems to be a general phenomenon in ESI-MS analysis of noncovalent complexes [7, 9, 23–25].

Among the parameters that are critical to ensure that as little fragmentation as possible occur during the electrospray process are the potentials applied to accelerate and collide the ions with gas in the electrospray interface. A concern was that increasing the potential between the desolvation capillary exit and the first skimmer (called CapExit), a prerequisite to observe the ions, could lead to fragmentation of the protein-ligand complex. As shown in Figure 2, varying this potential on a range from 200 to 400 V does not significantly alter the ratio of bound versus apo-complexes. To limit such effects nevertheless, the value chosen for the measurements (250 V) was the lowest that provided sufficient S/N ratios. A similar series of measurements varying the desolvation gas temperature led to the conclusion to leave the typical temperature used in the interface (140 °C) unchanged. The conservation of interactions in the protein-ligand complex over a broad range of conditions in the electrospray interface of the instrument indicates that there is no partial decomposition of the protein-ligand complex in the gas phase induced by these conditions, although it does not completely rule out such decompositions occurring at other stages of the electrospray process.

As free and ligand-bound forms of CK displayed different charge state distributions, the R values in our

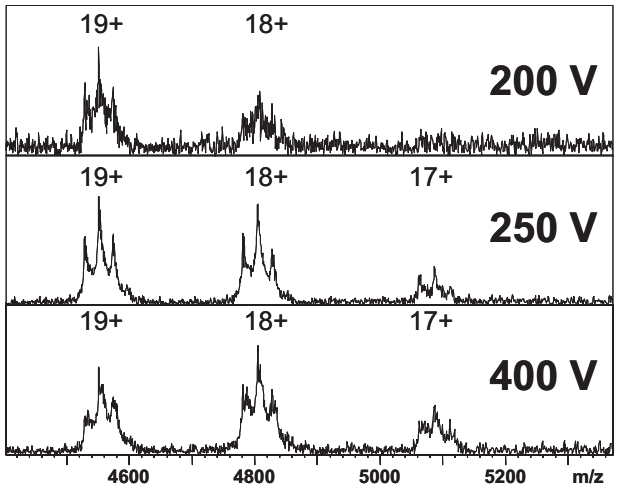

Figure 2. Dependence of interaction between CK (4 μM) and ADP (20 μM) on the CapExit voltage. The number above the peaks indicates the charge state, the CapExit voltage is shown on the right hand side of each spectrum.

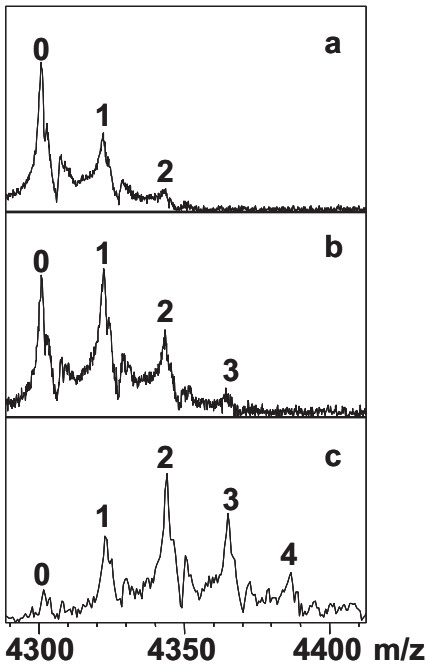

Figure 3. Titration of 4 μM CK with ADP. Numbers of ligands bound are indicated above the peaks. (**a**) 20+ charge state of 4 μM CK + 4 μM ADP; (**b**) 20+ charge state of 4 μM CK + 12 μM ADP; (**c**) 20+ charge state of 4 μM CK + 60 μM ADP.

spectra were calculated as the sum of peak heights (at all charge states) of the CK-ADP complexes in question, divided by the sum of peak heights (at all charge states) of the apo-protein (free CK), following the approach taken by Wang and coworkers [9]. As the intensity of ion signals in ICR spectra is proportional to the ion charge [26], this approach also included a correction of the intensities by dividing the signal intensity by the charge [9]. The intensities of the ligand-bound form of the protein had to be further corrected as their peak positions matched those of the adduct peak observed in the spectrum of the free protein (visualized by the right-hand star in the inset of Figure 1). It was assumed that this adduct peak was also present in the ligand-bound forms of the protein and did not influence ligand-binding.

When ADP was added at equimolar concentration to the CK solution, a maximum of two attached ligands were observed (Figure 3a). This is in agreement with the fact that CK has two active sites that can interact with ADP. When the ligand concentration was increased to 12 μM (corresponding to a 1:3 M ratio of CK:ADP), a low intensity peak appeared corresponding to CK with three bound ADP (Figure 3b). At 60 μM ADP (a 1:15 M ratio of CK:ADP) a maximum of four ADP were bound to CK (Figure 3c). These results could not simply be explained by a model with merely two specific binding sites.

The titration was performed with 4 μM CK and ligand concentrations ranging from 1 μM to 60 μM ADP (Table 1). Experiments were performed three times to check for variation between individual measurements as has been reported for nanoESI-MS of protein-carbohydrate complexes [9]. For the CK-ADP interaction, R_i values did not show substantial differences between individual experiments (data not shown), as indicated by the relative low standard deviation (Table 1). The experimental error in the measure of the R_i values increased with ligand concentration, which was expected as the intensity of the free protein decreases with increasing ligand concentration, increasing the error in calculation of the R_i values.

A possible explanation for these data would be the occurrence of some nonspecific binding added to the two specific binding sites present on the protein as known from other work on this system [15, 19]. However, it is not possible to corroborate this hypothesis by visual inspection of the experimental data alone.

To investigate this hypothesis, a first element is to rule out that the binding stemmed from entirely statistical binding on more than two sites (which means that there are not as expected two specific sites with a larger affinity than other sites on the protein). The experimentally obtained R_i values at each ligand concentration were compared with a statistical distribution on an unknown number of binding sites that can be calculated according to eq 5. The result shows that the experimental data cannot be interpreted as nonspecific interac-

Table 1. Experimental ratios and average number of bound ligands for the system CK + ADP. Values as well as errors correspond to the average of three individual measurements

$[ADP]_0/\mu M$	R_1	R_2	R_3	R_4	$\bar{I}$
1	0.06 ± 0.04	-	-	-	0.05 ± 0.03
2	0.14 ± 0.05	0.01 ± 0.01	-	-	0.13 ± 0.05
4	0.31 ± 0.06	0.02 ± 0.02	-	-	0.27 ± 0.06
6	0.45 ± 0.04	0.09 ± 0.02	-	-	0.41 ± 0.03
8	0.56 ± 0.03	0.14 ± 0.02	-	-	0.49 ± 0.04
10	0.74 ± 0.05	0.22 ± 0.03	-	-	0.60 ± 0.04
12	0.80 ± 0.04	0.29 ± 0.05	0.02 ± 0.01	-	0.69 ± 0.05
16	1.13 ± 0.04	0.57 ± 0.09	0.10 ± 0.01	-	0.92 ± 0.04
20	1.33 ± 0.05	0.70 ± 0.15	0.16 ± 0.03	-	1.01 ± 0.06
40	2.73 ± 0.25	2.73 ± 0.44	0.87 ± 0.17	0.24 ± 0.05	1.55 ± 0.09
60	3.61 ± 0.85	5.02 ± 1.24	2.20 ± 0.90	0.90 ± 0.09	1.87 ± 0.16

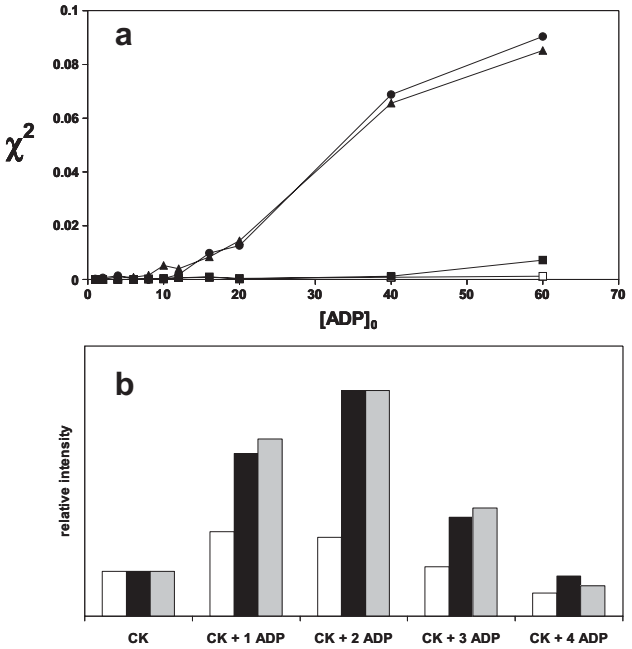

Figure 4. (**a**) Deviation of experimentally obtained spectra from spectra obtained by fitting with different models (filled circles: only specific interactions with two specific binding sites are considered (eq 4); filled triangles: only nonspecific interactions on a large number of binding sites are considered (eq 5); filled squares: model based on two specific and two nonspecific interaction sites (eq 8, first part, with s = 2 and n = 2); open squares: model based on two specific and a large number of nonspecific interaction sites (eq 8, last part, with s = 2). At a given concentration of ADP, the χ^2 value represents the sum of the squares of the differences between experimental and calculated intensities divided by the total intensity. (**b**) The dataset 4 μM CK + 60 μM ADP fitted with different models (black bars: experimental data, white bars: only nonspecific interaction sites taken into account; grey bars: two specific and a large number of nonspecific interaction sites taken into account).

tions alone (Figure 4a, filled triangles, Figure 4b, white bars).

The experimental data should thus be considered to represent a superposition of at least two different types of protein-ligand interactions. The simplest hypothesis is to assume that one can be related to the specific binding of ligands in the active site of the enzyme and the other to nonspecific binding of ligands probably attached during the electrospray process. It is of interest to separate the contributions of these two types of interactions, since only the specific binding to the catalytic site has to be taken into account for the evaluation of the solution phase binding constants. The model developed in the "Experimental" section, which should be general enough to be applied to other cases for which nonspecific binding is observed, is based on the deconvolution of two statistical distributions, the first (named "specific") limited to a finite number of binding sites known a priori, the second (named "nonspecific") can either be applied to a defined number of binding sites or to an unknown number of binding sites in the case where this number is large enough and provided that there are few ligands bound to these sites.

As for the specific interactions, CK has been shown to be a protein for which the two binding sites are equivalent and independent under the experimental conditions employed in our study [17, 19, 27]. The distribution of ligands in the binding sites can therefore be described by a binomial distribution on two sites according to eq 4.

As for the nonspecific fraction of the interaction, the origin is less clear: there is some evidence that it could be related to the electrospray process used for the production of ions [7, 10]. Considering the charge residue model (CRM) originally proposed by Dole and coworkers [28] that is likely to be valid for the ion formation in the electrospray source for large biomolecules [29], one could assume aggregation of ligands to the protein in the course of the evaporation of a finite size droplet in the electrospray source in the final stages of the droplet evaporation process. Considering that the ligand concentration is small enough, the Poisson distribution is a good approximation for analyzing the resulting data. Similar Poisson distributions have been observed for purely nonspecific interactions [10].

If the nonspecific binding occurred in solution by the interaction of the ligands with the surface of the protein before the electrospray process, there could be a limited number of available binding sites. However, there is little evidence for means to determine this number of sites. Increasing the concentration of ligand above 80 μM leads to the observation of a fifth and sixth ligand binding, which shows that at least four supplementary binding sites should be considered.

A model based on the presence of two specific and of only two nonspecific binding sites (Figure 4a, filled squares) gave a much better fit of the experimental data than with nonspecific interactions alone. However, at ligand concentrations above 40 μM, where nonspecific binding is most likely to occur, this model still gave a poor fit. An increase in the number of nonspecific binding sites to 10 resulted in a fit (data not shown) that was of the same quality as the fit obtained by applying the model based on two specific binding sites and the Poisson approximation for nonspecific binding (Figure 4a, open squares): these two models differ by less than 2% on the values of the binding constants. In light of the low occupancy of the ligand binding sites ($\bar{l}$ = 1.87 at 60 μM), the Poisson distribution as employed in the deconvolution model is thus a good approximation for the nonspecific binding, with the advantage that using a Poisson distribution does not require an a priori knowledge of the number of ligands that are nonspecifically bound.

The deconvolution model detailed in the Experimental section has therefore been applied to the experimental data obtained for the CK + ADP system with $\bar{s}$ = 2 and with the Poisson distribution approximation for the nonspecific binding. The $\bar{s}$ parameter was adjusted so that the R_i values given by eq 8 fitted the experimental ratios given in Table 1. Once this is done, one can apply

Table 2. Data obtained after deconvolution of specific and non-specific interactions. Values in parenthesis for R_1^*, R_2^*, $K_{1,diss}$ and $K_{2,diss}$ are those used to check the consistency of the model (see text). Errors for R_1^*, R_2^*, $K_{1,diss}$ and $K_{2,diss}$ are derived from equations 6, 3, and 1 assuming that the error on $\bar{s}$ and $\bar{n}$ is equal to the error on $\bar{I}$

$[ADP]_0$/ μM	$\bar{s}$	$\bar{n}$	R_1^*	R_2^*	$K_{1,diss}/\mu M$	$K_{2,diss}/\mu M$	$K_{2,diss}/K_{1,diss}$
1	0.05	—	0.05 (0.06) ± 0.03	—	14.4 (14.0) ± 34.0	—	—
2	0.12	0.00(5)	0.13 (0.13) ± 0.06	0.004 (0.004) ± 0.002	11.3 (11.2) ± 8.4	—	—
4	0.26	0.00(3)	0.30 (0.30) ± 0.10	0.02 (0.02) ± 0.01	9.7 (9.7) ± 3.5	—	—
6	0.27	0.14	0.36 (0.35) ± 0.06	0.03 (0.04) ± 0.01	14.0 (13.7) ± 2.5	56 (47) ± 55	4.0 (3.4)
8	0.33	0.16	0.46 (0.46) ± 0.09	0.05 (0.06) ± 0.01	14.3 (14.0) ± 1.3	57 (48) ± 22	4.0 (3.4)
10	0.46	0.14	0.69 (0.68) ± 0.11	0.10 (0.12) ± 0.02	11.9 (11.7) ± 1.1	48 (44) ± 19	4.0 (3.7)
12	0.43	0.26	0.71 (0.70) ± 0.14	0.10 (0.15) ± 0.02	14.7 (14.1) ± 1.2	59 (46) ± 27	4.0 (3.3)
16	0.55	0.37	1.10 (1.09) ± 0.15	0.21 (0.30) ± 0.03	12.6 (12.1) ± 0.6	50 (48) ± 22	4.0 (4.0)
20	0.66	0.34	1.4 (1.4) ± 0.3	0.34 (0.41) ± 0.07	12.4 (12.1) ± 0.7	50 (57) ± 36	4.0 (4.7)
40	1.10	0.45	3.8 (3.6) ± 1.0	2.34 (2.48) ± 0.64	9.2 (9.9) ± 0.8	37 (50) ± 16	4.0 (5.1)
60	1.25	0.63	6.3 (5.6) ± 3.1	5.2 (5.4) ± 2.6	8.9 (9.8) ± 1.8	35 (56) ± 29	4.0 (5.7)

directly eq 3 as outlined in the Experimental section to calculate the fitted ratios (Table 2). $K_{1,diss}$ and $K_{2,diss}$ are the sequential dissociation constants for the equilibria CK-ADP ⇄ CK + ADP and CK-ADP_2 ⇄ CK-ADP + ADP, respectively.

However, application of the deconvolution model leads to values of $K_{1,diss}$ and $K_{2,diss}$ that are, by inherent definitions of the model (noncooperative binding), in a fixed ratio of 4, thus not allowing for any analysis of the validity of the model. The quality of the results was thus evaluated by partially deconvoluting the experimental ratios, removing the nonspecific contribution ($\bar{n}$) from the experimental ratios (bearing in mind that, for instance, $R_1 = R_1^1 + \bar{n}$). $K_{1,diss}$ and $K_{2,diss}$ were then calculated based on these corrected experimental ratios (Table 2, values in parenthesis) instead of using the purely fitted ratios. Within this latter approach, a flaw in the assumptions of the model would manifest itself by significant deviations from expected outcomes. For example, cooperativity between both sites (being contradictory to the assumptions underlying our model) would lead to a significant deviation in the ratio $K_{2,diss}/K_{1,diss}$, that is expected to be 4 in the complete absence of cooperativity. The values presented in parenthesis in Table 2 are obtained by following the latter approach.

It is of interest to notice that the individual contribution of each different type of species (specific and nonspecific) can be computed according to eq 6. This allows giving an example of the deconvolution process based on the 4 μM CK + 60 μM ADP experimental data (Figure 5). Each experimental peak can be divided into a sum of different contributions (black: no specifically bound ligand, R_i^0; grey: one specifically bound ligand, R_i^1; white: two specifically bound ligands, R_i^2). This figure also shows that the nonspecific binding accounts for about 50% of the protein-two ligand intensity. This would have led to a completely underestimated dissociation constant if the deconvolution model had not been used.

The data obtained by applying the deconvolution model to the experimental data are in good agreement with the experimental data (Figure 4a, filled squares, Figure 4b grey bars), especially at higher concentrations where the fraction of nonspecific binding is most likely to increase. The average dissociation constants calculated from the fitted data in the ligand range from 1 to 60 μM ADP are $K_{1,diss,ADP}$ = 11.8 ± 1.5 μM and $K_{2,diss,ADP}$ = 48 ± 6 μM, respectively. The ratio of $K_{2,diss,ADP}/K_{1,diss,ADP}$ is of course of 4 in the case where the model is strictly applied as expected for two equivalent and independent binding sites according to the multi-equilibrium formalism for noncooperative binding sites [9, 30]. In parenthesis, one can see that the ratio does not deviate significantly from 4 within the error margin when one simply removes nonspecific contributions, removing some constraints from the model. The poor quality of the measurement of $K_{2,diss}$ at the highest concentrations arises from the fact that the intensity of the peak corresponding to the apo-protein decreases with increasing concentrations, leading to an increase in the error on the measurement of the ratios for individual measurements. However, as stated above, R_i values did not vary dramatically between different series of experiments. The K_d values obtained by our method are of the same order of magnitude as the reported litera-

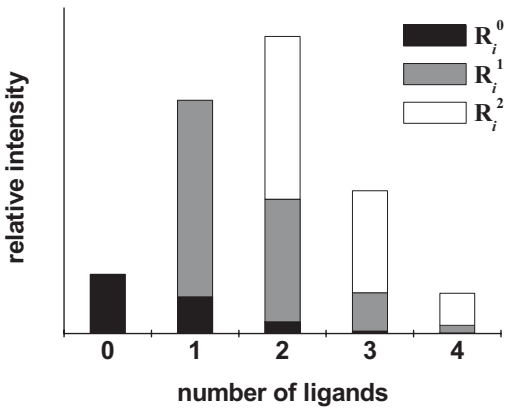

Figure 5. Contributions of species with zero specifically bound ligands (black), one specifically bound ligand (grey), and two specifically bound ligands (white), to the experimental intensities of 4 μM CK incubated with 60 μM ADP.

ture values of about $K_1 = 50\ \mu M$ and $K_2 = 200\ \mu M$ that were obtained in the absence of other ligands than the one in question [17, 20]. Different experimental conditions most probably account for the remaining difference with respect to the literature values. The data obtained by applying our model agree with two noncooperative binding sites of CK for ADP under the experimental conditions employed: the model assumes noncooperativity between the two sites, but as discussed above, a deviation of the ratio $K_{2,diss,ADP}/K_{1,diss,ADP}$ could be expected if the model was not valid. This does not completely rule out the presence of weak cooperativity between the sites since in this case the deviation from our noncooperative model would be well below the experimental error margin. However, a strong cooperativity between the binding sites would have led to a poor fit with significant deviations. There might also be other experimental conditions (e.g., solution composition) where the sites behave in a cooperative manner [17].

The nonspecific binding, as characterized by $\bar{n}$, increases with the ligand concentration and contributes to 25–40% (from as low as 6 μM ADP concentration) of the total binding. Interestingly, already at a protein:ligand ratio of 1:3, the nonspecific interactions contribute to 38% of the overall ligand binding (Table 2). In the spectrum, the experimental indication for nonspecific binding to occur is only a small peak corresponding to CK with three bound ligands (Figure 3b). Our result shows that nonspecific interactions also contribute to the peak corresponding to CK with one and two ligands bound, respectively, and can thus not be neglected. Therefore, already at relatively low ligand concentration, nonspecific binding should be taken into consideration.

As the model was built around the CK/ADP system, we subsequently aimed at studying the CK/ATP interaction to further validate our approach. ATP is a second physiological ligand of CK and as it is chemically similar to ADP, it was expected to show similar behaviour during the ESI experiments. The ESI mass spectra of CK titrated with ATP show the same charge state distribution as the uncomplexed dimer, and exhibit no dissociation of the ligand upon varying the capillary exit voltage (data not shown). In the mass spectrum, peaks appeared that were attributed to ATP-bound CK (Figure 6). For a given ligand concentration, the extent of ATP binding to the protein was significantly lower than the extent of ADP binding, as indicated by the lower abundance of peaks attributed to ligand-bound protein. As in the case of ADP, upon increasing the concentration of ATP, observation of a peak corresponding to CK having three bound ATP provides clear experimental evidence for nonspecific binding (Figure 6c).

The data obtained upon titration of CK with ATP were analyzed by applying our deconvolution model (Table 3). For each data point, the model gave a good fit within the experimental error range (data not shown). The final data argue, as was the case for ADP, for the presence of nonspecific interactions from as low as 12 μM on, where there is no experimental evidence for this binding mode (Table 3, Figure 6).

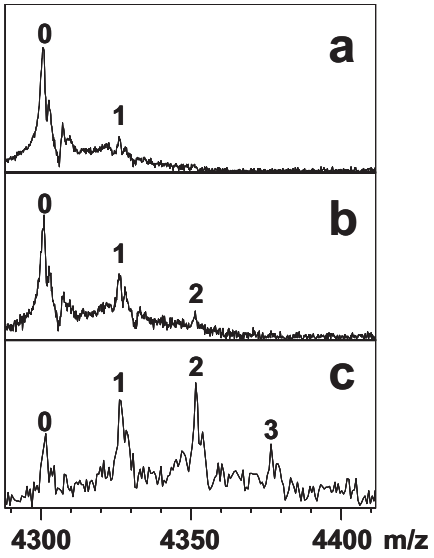

Figure 6. Titration of 4 μM CK with ATP. Numbers of ligands bound are indicated above the peaks. (**a**) 20+ charge state of 4 μM CK + 4 μM ATP; (**b**) 20+ charge state of 4 μM CK + 12 μM ATP; (**c**) 20+ charge state of 4 μM CK + 60 μM ATP.

The binding constants for the CK/ATP interaction obtained after application of our model are $K_{1,diss,ATP} = 27 \pm 7\ \mu M$ and $K_{2,diss,ATP} = 114 \pm 27\ \mu M$, respectively, assuming that there is no cooperativity. The constants obtained by the MS approach are thus significantly smaller than those reported (K_{diss} = 300–500 μM). These differences are most probably due to the different experimental setup and conditions employed. However, MS analysis and deconvolution of specific and nonspecific interactions display the correct qualitative order of the interaction constants ($K_{diss,ADP} < K_{diss,ATP}$).

The data obtained allow for direct comparison of the average number of nonspecific interactions in either case. A simple plot of $\bar{n}$ versus $[L]_{eq}$ (L = ADP, ATP) shows that the two ligands show a similar behavior in the experimental error range (Figure 7). In either case, the average number of nonspecific interactions increases with increasing ligand concentration.

These data show another important result obtained by the application of our deconvolution model: the degree of nonspecific binding in less sensitive to the kind of ligand than the specific binding mode. As ADP and ATP differ by only one phosphate group, they are not expected to behave very differently with respect to the nonspecific binding mode. The specific binding, on the other hand, varies significantly between the two ligands (Tables 2 and 3), and thus is very likely to reflect the solution binding affinity.

As for the origin of the nonspecific interactions, there are two possible sources: they may be generated during the electrospray process or they can already be present in solution. In either case, simple models for the formation of these nonspecific adducts (droplet evaporation

Table 3. Experimental and fitted data obtained after titration of CK with ATP

$[ATP]_0/\mu M$	R_1	R_2	R_3	R_4	$\bar{I}$
1	0.03 ± 0.03	-	-	-	0.03 ± 0.03
2	0.09 ± 0.02	-	-	-	0.08 ± 0.02
4	0.16 ± 0.04	-	-	-	0.14 ± 0.03
6	0.22 ± 0.02	-	-	-	0.18 ± 0.05
8	0.35 ± 0.03	0.02 ± 0.02	-	-	0.29 ± 0.03
10	0.40 ± 0.10	0.04 ± 0.02	-	-	0.34 ± 0.07
20	0.72 ± 0.09	0.23 ± 0.03	-	-	0.60 ± 0.04
30	0.87 ± 0.15	0.33 ± 0.09	-	-	0.69 ± 0.08
40	1.08 ± 0.29	0.61 ± 0.14	0.14 ± 0.03	-	0.96 ± 0.08
60	1.64 ± 0.37	1.29 ± 0.36	0.36 ± 0.18	0.10 ± 0.01	1.30 ± 0.16

$[ATP]_0/\mu M$	$\bar{s}$	$\bar{n}$	R_1*	R_2*	$K_{1,diss}/\mu M$	$K_{2,diss}/\mu M$
1	0.03	0.00	0.03 ± 0.03	-	-	-
2	0.08	0.00	0.08 ± 0.02	-	20 ± 6	-
4	0.14	0.00	0.15 ± 0.04	-	24 ± 7	-
6	0.18	0.00	0.20 ± 0.08	0.01 ± 0.004	26 ± 11	104 ± 45
8	0.29	0.00	0.34 ± 0.06	0.02 ± 0.005	20 ± 4	82 ± 15
10	0.32	0.02*	0.39 ± 0.13	0.04 ± 0.01	23 ± 8	90 ± 33
20	0.43	0.17	0.66 ± 0.11	0.09 ± 0.01	28 ± 4	111 ± 18
30	0.52	0.18	0.83 ± 0.23	0.14 ± 0.04	34 ± 9	135 ± 35
40	0.44	0.52	0.95 ± 0.28	0.13 ± 0.04	40 ± 11	162 ± 45
60	0.68	0.62	1.91 ± 0.96	0.49 ± 0.25	30 ± 14	120 ± 57

or multiple equilibria with many sites and identical binding constants) would result in a linear dependence of the average number of bound ligands $\bar{n}$ versus the free ligand concentration [10]. However, the relatively large error in the value of $\bar{n}$ does not allow for a detailed discussion of this point. It is thus not generally possible to address the question of the origin or the exact nature of the nonspecific interactions. These elements might already point to the limits of the modeling of the nonspecific interactions as presented in our deconvolution model. To precisely take into account any possible process leading to the formation of nonspecific interactions in the deconvolution model, more adjustable parameters would be required. However, a deconvolution model with only one adjustable parameter, as employed in the present study, seemed to be reasonable in light of the experimental data.

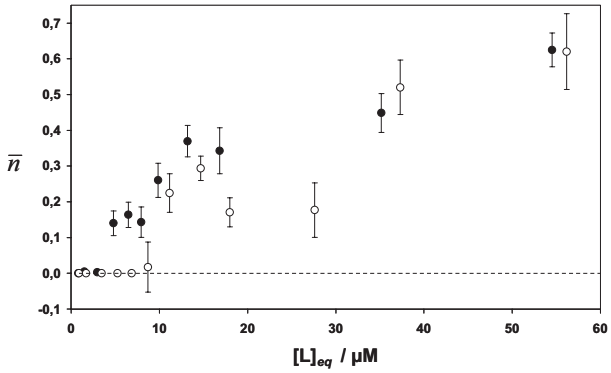

Figure 7. Average number of nonspecific interactions as a function of free ligand concentration for the CK/ADP (filled circles) and CK/ATP equilibria (open circles), respectively.

Conclusions

The study of noncovalent interactions by electrospray mass spectrometry is hampered by the presence of nonspecific interactions already present in solution or formed during the electrospray process [10]. The propensity of forming nonspecific interactions increases with ligand concentration. Thus, by using the titration method [9], one should work with low ligand concentration to minimize the influence of nonspecific binding. However, when studying systems with large dissociation constants (10^{-5} to 10^{-3} M), it is necessary to increase ligand concentration above a certain threshold value to observe the formation of complexes. Using the deconvolution model presented here, it should be possible to increase the range of ligand concentration about 10-fold. The approach taken by us allows for separation of specific and nonspecific interactions. The model allows to calculate equilibrium constants containing only the contribution from specific interactions. The model is limited to systems for which there is initial knowledge of the specific interactions that are expected. In its present form, it is limited to systems with binding sites that show no cooperativity, i.e., that are equivalent and independent. By introducing the ratio of constants as an additional parameter, it would be possible to extend the model for systems that show cooperativity. However, with an increasing number of adjustable parameters, the quality of the MS data (especially the S/N ratio) becomes even more important. Fitting experimental data to a model containing only one adjustable parameter (in our case the average number of specifically bound ligands, $\bar{s}$) does not impose this constraint.

References

1. Fenn, J. B.; Mann, M.; Meng, C. K.; Wong, S. F.; Whitehouse, C. M. Electrospray Ionization for Mass Spectrometry of Large Biomolecules. *Science* **1989**, *246*, 464–471.
2. Loo, J. A. Electrospray Ionization Mass Spectrometry: A Technology for Studying Noncovalent Macromolecular Complexes. *Int. J. Mass. Spectrom.* **2000**, *200*, 175–186.
3. Veenstra, T. D. Electrospray Ionization Mass Spectrometry in the Study of Biomolecular Noncovalent Interactions. *Biophys. Chem.* **1999**, *79*, 63–79.
4. Daniel, J. M.; Friess, S. D.; Rajagopalan, S.; Wendt, S.; Zenobi, R. Quantitative Determination of Noncovalent Binding Interactions Using Soft Ionization Mass Spectrometry. *Int. J. Mass Spectrom.* **2002**, *216*, 1–27.
5. Smith, R. D. Evolution of ESI-Mass Spectrometry and Fourier Transform Ion Cyclotron Resonance for Proteomics and Other Biological Applications. *Int. J. Mass Spectrom.* **2000**, *200*, 509–544.
6. Heck, A. J. R.; Jørgensen, T. J. D. Vancomycin in Vacuo. *Int. J. Mass Spectrom.* **2004**, *236*, 11–23.
7. Robinson, C. V.; Chung, E. W.; Kragelund, B. B.; Knudsen, J.; Aplin, R. T.; Poulsen, F. M.; Dobson, C. M. Probing the Nature of Noncovalent Interactions by Mass Spectrometry. A Study of Protein-CoA Ligand Binding and Assembly. *J. Am. Chem. Soc.* **1996**, *118*, 8646–8653.
8. Peschke, M.; Verkerk, U. H.; Kebarle, P. Features of the ESI Mechanism that Affect the Observation of Multiply Charged Noncovalent Protein Complexes and the Determination of the Association Constant by the Titration Method. *J. Am. Soc. Mass Spectrom.* **2004**, *15*, 1424–1434.
9. Wang, W.; Kitova, E. N.; Klassen, J. S. Determination of Protein-Oligosaccharide Binding by Nanoelectrospray Fourier-Transform Ion Cyclotron Resonance Mass Spectrometry. *Methods Enzymol.* **2003**, *362*, 376–396.
10. Wang, W.; Kitova, E. N.; Klassen, J. S. Nonspecific Protein-Carbohydrate Complexes Produced by Nanoelectrospray Ionization. Factors Influencing Their Formation and Stability. *Anal. Chem.* **2005**, *77*, 3060–3071.
11. Wang, W.; Kitova, E. N.; Sun, J.; Klassen, J. S. Blackbody Infrared Radiative Dissociation of Nonspecific Protein-Carbohydrate Complexes Produced by Nanoelectrospray Ionization: The Nature of the Noncovalent Interactions. *J. Am. Soc. Mass Spectrom.* **2005**, *16*, 1583–1594.
12. Pinske, M. W. H.; Heck, A. J. R.; Rumpel, K.; Pullen, F. Probing Noncovalent Protein-Ligand Interactions of the cGMP-Dependent Protein Kinase Using Electrospray Ionization Time of Flight Mass Spectrometry. *J. Am. Soc. Mass Spectrom.* **2004**, *15*, 1392–1399.
13. Sundquist, G.; Benkestock, K.; Roeraade, J. Investigation of Multiple Binding Sites on Ribonuclease A Using Nano-Electrospray Ionization Mass Spectrometry. *Rapid Commun. Mass Spectrom.* **2005**, *19*, 1011–1016.
14. Benkestock, K.; Edlund, P.-O.; Roeraade, J. Electrospray Ionization Mass Spectrometry as a Tool for Determination of Drug Binding Sites to Human Serum Albumin by Noncovalent Interaction. *Rapid Commun. Mass Spectrom.* **2005**, *19*, 1637–1643.
15. Watts, D. C. Creatine Kinase (Adenosine 5′-Triphosphate-Creatine Phosphotransferase). In *The Enzymes*, Vol. VIII; Boyer, P. D., Ed.; Academic Press: New York/London, 1973; pp 383–455.
16. Borders, C. L.; Snider, M. J.; Wolfenden, R.; Edminston, P. L. Determination of the Affinity of Each Component of a Composite Quaternary Transition-State Analogue Complex of Creatine Kinase. *Biochemistry* **2002**, *41*, 6995–7000.
17. McLaughlin, A. C. The Interaction of 8-Anilino-1-Nnaphtalenesulfonate with Creatine Kinase. *J. Biol. Chem.* **1974**, *249*(5), 1445–1452.
18. Burbaum, J. J.; Knowles, J. R. Internal Thermodynamics of Enzymes Determined by Equilibrium Quench: Values of Kint for Enolase and Creatine Kinase. *Biochemistry* **1989**, *28*, 9306–9317.
19. Hornemann, T.; Rutishauser, D.; Wallimann, T. Why is Creatine Kinase a Dimer? Evidence for Cooperativity Between the Two Subunits. *Biochim. Biophys. Acta* **2000**, *1480*(1/2), 365–373.
20. Kuby, S. A.; Mahowald, T. A.; Noltmann, E. A. Studies on Adenosine Triphosphate Transphosphorylases. IV. Enzyme-Substrate Interactions. *Biochemistry* **1962**, *1*, 748–762.
21. Loo, J. A.; Ogorzalek Loo, R. G. Electrospray Ionization Mass Spectrometry of Peptides and Proteins. In *Electrospray Ionization Mass Spectrometry*. Cole, R. B., ed. John Wiley and Sons, Inc.: New York, 1997, pp. 385–419.
22. Chowdhury, S. K.; Katta, V.; Chait, B. T. Probing Conformational Changes in Proteins by Mass Spectrometry. *J. Am. Chem. Soc.* **1990**, *112*, 9012–9013.
23. Loo, J. A.; Hu, P.; McConnell, P.; Mueller, W. T.; Sawyer, T. K.; Thanabal, V. A Study of Src SH2 Domain Protein-Phosphopeptide Binding Interactions by Electrospray Ionization Mass Spectrometry. *J. Am. Soc. Mass Spectrom*. **1997**, *8*, 234–243.
24. Greig, M. J.; Gaus, H.; Cummins, L. L.; Sasmor, H.; Griffey, R. H. Measurement of Macromolecular Binding Using Electrospray Mass Spectrometry. Determination of Dissociation Constants for Oligonucleotide-Serum Albumin Complexes. *J. Am. Chem. Soc.* **1995**, *117*, 10765–10766.
25. Gabelica, V.; De Pauw, E.; Rosu, F. Interaction between Antitumor Drugs and a Double-Stranded Oligonucleotide Studied by Electrospray Ionization Mass Spectrometry. *J. Mass Spectrom.* **1999**, *34*, 1328–1337.
26. Jurchen, J. J.; Garcia, D. E.; Williams, E. R. Further Studies on the Origins of Asymmetric Charge Partitioning in Protein Homodimers. *J. Am. Soc. Mass Spectrom.* **2004**, *15*, 1408–1415.
27. Forstner, M.; Kriechbaum, M.; Laggner, P.; Wallimann, T. Structural Changes of Creatine Kinase Upon Substrate Binding. *Biophys. J.* **1998**, *75*, 1016–1023.
28. Dole, M.; Mack, L. L.; Hines, R. L.; Mobley, R. C.; Ferguson, L. D.; Alice, M. B. Molecular Beams of Macro-Ions. *J. Chem. Phys.* **1968**, *49*, 2240–2249.
29. Kebarle, P; Ho, Y. On the Mechanism of Electrospray Mass Spectrometry. In *Electrospray Ionization Mass Spectrometry*. Cole, R. B., ed. John Wiley and Sons, Inc.: New York, 1997, pp. 3–63.
30. Tanford, C. Multiple Equilibria. In *Physical Chemistry of Macromolecules*. Tanford, C., ed. John Wiley and Sons, Inc.: New York/London, 1961, pp. 526–586.